

Supplementary Materials: Photocatalytic Conversion of Organic Pollutants in Air: Quantum Yields Using a Silver/Nitrogen/TiO₂ Mesoporous Semiconductor under Visible Light

Adilah Sirivallop ^{1,2}, Salvador Escobedo ³, Thanita Areerob ⁴, Hugo de Lasa ^{3,*} and Siriluk Chiarakorn ^{5,*}

- ¹ Division of Environmental Technology, The Joint Graduate School of Energy and Environment, King Mongkut's University of Technology Thonburi, Bangkok 10140, Thailand; adey.sirivallop@gmail.com
 - ² Center of Excellence on Energy Technology and Environment (CEE), PERDO, Ministry of Higher Education, Science, Research, and Innovation, Bangkok 10140, Thailand
 - ³ Chemical Reactor Engineering Centre (CREC), Faculty of Engineering, Department of Chemical and Biochemical Engineering, University of Western Ontario, London, ON N6A 5B9, Canada; sescobe@uwo.ca
 - ⁴ Faculty of Technology and Environment, Prince of Songkla University, Phuket Campus, Phuket 83120, Thailand; Thanita.a@phuket.psu.ac.th
 - ⁵ Environmental Technology Program, School of Energy, Environment and Materials, King Mongkut's University of Technology Thonburi, Bangkok 10140, Thailand; siriluk.chi@kmutt.ac.th
- * Correspondence: hdelasa@uwo.ca (H.d.L.); siriluk.chi@kmutt.ac.th (S.C.)

Supplementary A: GC-FID Program Method

The GC-FID program method equipped with a packed Poropak Q column (2 m column length, 2 mm ID inner diameter, and 2 μm film thickness) was used for monitoring the concentration of methanol, CO₂, formaldehyde, and formic acid. Helium gas was used as the carrier gas with a flow rate of 15 mL/min. The oven temperature was programmed from 75 °C to 210 °C at 40 °C/min, and held for 6.50 min for the duration of the separation (see Figure S1).

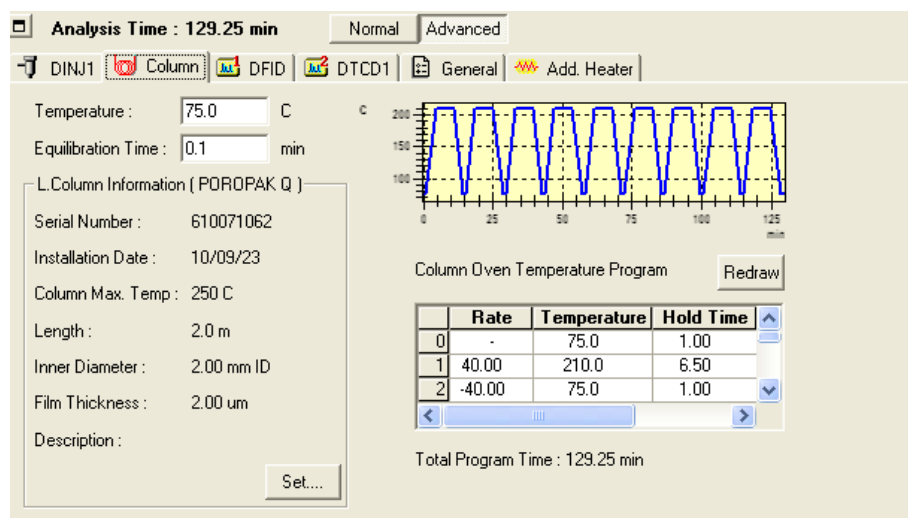


Figure S1. GC parameters of the column separation method.

Supplementary B: Calibration Curves and GC Analysis

Figure S2 shows the analytical calibrations curves of a) methanol and (b) CO₂. Furthermore, in Figure S3 one can see the typical chromatogram from the GC-FID.

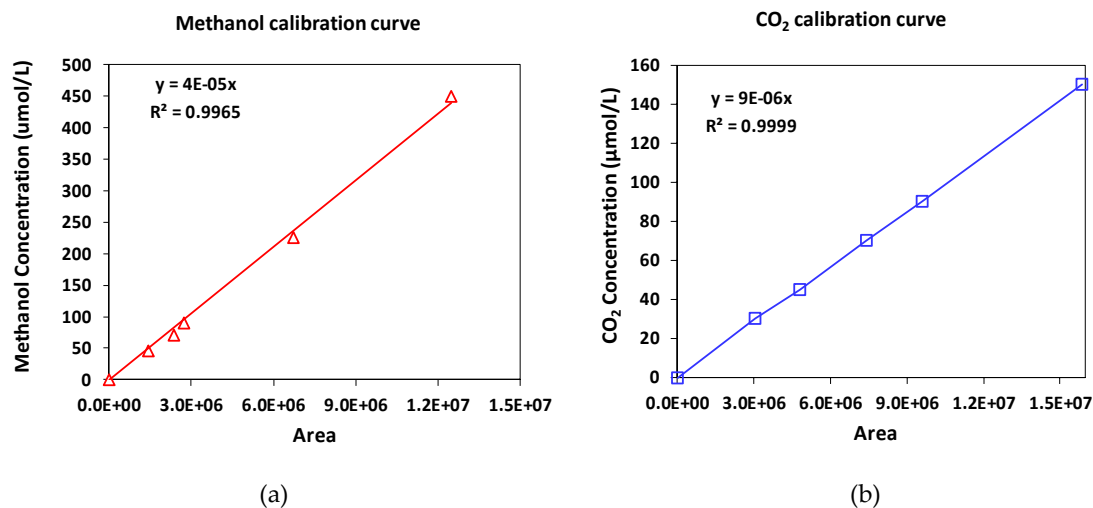


Figure S2. Calibration Curves for (a) methanol (0-450 µmol/L) and (b) CO₂ (0-150 µmol/L).

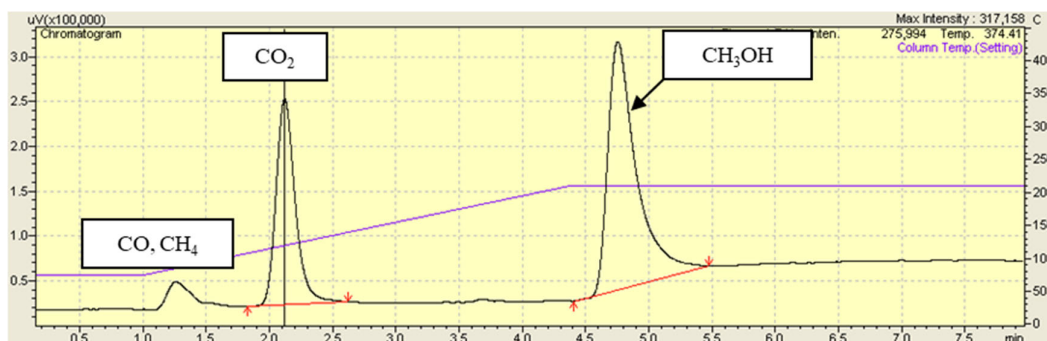
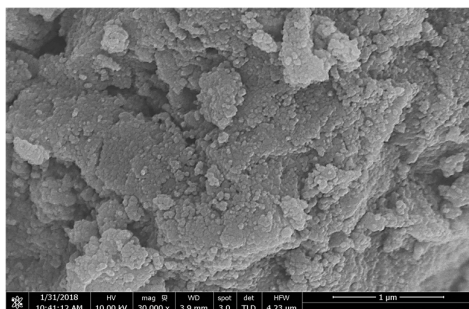


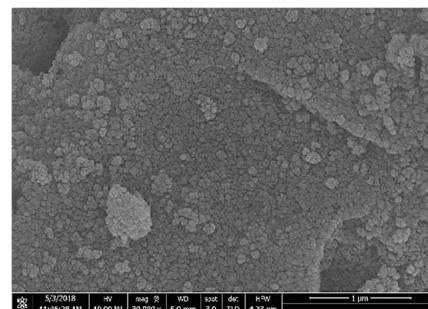
Figure S3. Typical Chromatograms for Methanol (CH₃OH) and CO₂ Obtained from a GC-FID.

Supplementary C: SEM and EDX Characterization

EDX analysis was performed on the synthesized photocatalyst together with SEM (see Figure S4a,b). The atomic ratio (at. %) and elemental mapping of individual species of N/Ag/TiO₂ photocatalyst are presented in Figure S4c and Figure S4d, respectively.



(a) Bare-TiO₂



(b) N/Ag/TiO₂

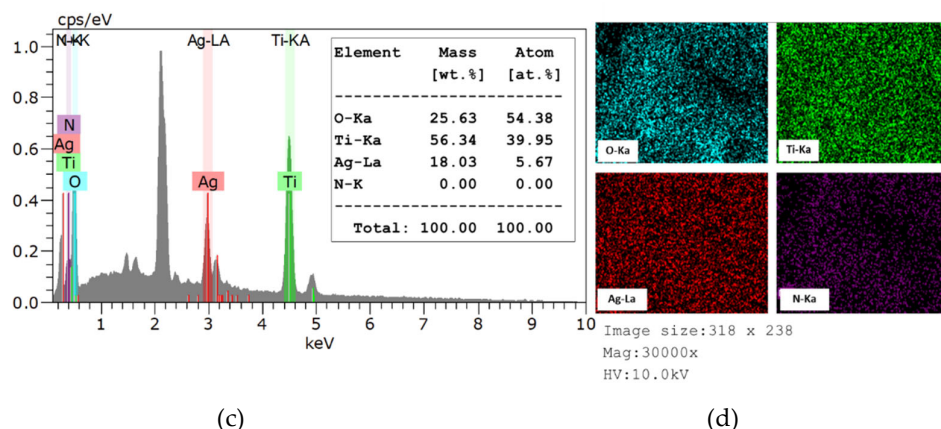


Figure S4. SEM images of (a) bare-TiO₂ and (b) N/Ag/TiO₂ photocatalysts. (c) EDX spectrum of N/Ag/TiO₂ photocatalyst. The inset table shows the compositional ratio of elemental O, Ti, Ag, N in N/Ag/TiO₂. (d) EDX mapping of elemental O, Ti, Ag and N in N/Ag/TiO₂ photocatalyst.

Supplementary D: Photoluminescence Analysis

The photoluminescence (PL) spectra of bare-TiO₂ and N/Ag/TiO₂ photocatalysts were analyzed using the LED lamp with a 354 nm wavelength as the excitation light source at room temperature and this to investigate the transfer behavior of photoexcited electron and hole and the rate of charge recombination of different photocatalyst.

Figure S5 reports the PL spectra of bare-TiO₂ and N/Ag/TiO₂ photocatalysts. It could be found that the bare-TiO₂ exhibits a strong and wide PL spectrum at the wavelength range from 300-800 nm. On the other hand, after the addition of Ag and N, the PL intensity of a N/Ag/TiO₂ photocatalyst was much lower compared to those of bare-TiO₂. This result suggests that the Ag and N has direct influence on the change in the electronic structure of the bare-TiO₂ photocatalyst, which is consistent with other [1,2].

In addition, according to the PL emission is directly related to the photoexcited electron and hole recombination rate, consequently the lower PL intensity in a N/Ag/TiO₂ photocatalyst indicates the reduction of photoexcited e⁻/h⁺ recombination rate. This phenomenon could be explained by the fact that the photoexcited electrons were trapped by Ag deposited on bare-TiO₂ surface acting as electron acceptors, whereas positive holes were trapped by N atoms [1,2].

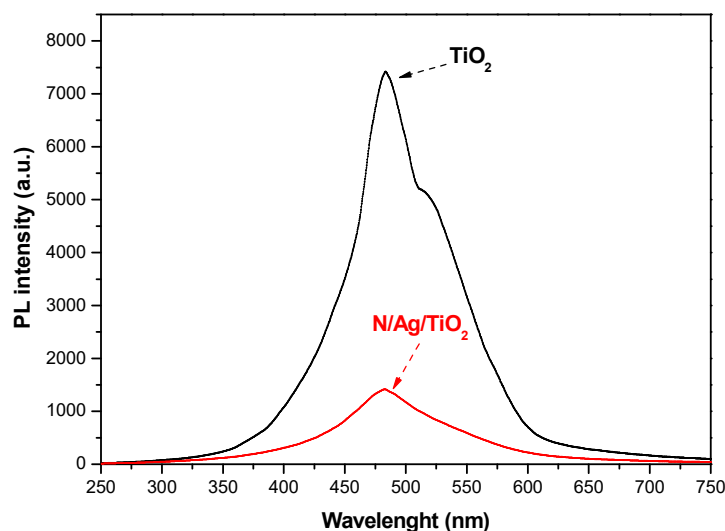


Figure S5. Photoluminescence (PL) spectra of bare-TiO₂ and N/Ag/TiO₂ photocatalysts.

References

1. Le, L.; Xu, J.; Zhou, Z.; Wang, H.; Xiong, R.; Shi, J. Effect of oxygen vacancies and Ag deposition on the magnetic properties of Ag/N co-doped TiO₂ single-crystal films. *Mater. Res. Bull.* **2018**, *102*, 337–341, doi:10.1016/j.materresbull.2018.01.045.
2. Devi, L.G.; Nagaraj, B.; Rajashekhar, K.E. Synergistic effect of Ag deposition and nitrogen doping in TiO₂ for the degradation of phenol under solar irradiation in presence of electron acceptor. *Chem. Eng. J.* **2012**, *181–182*, 259–266, doi:10.1016/j.cej.2011.11.076.